# A TWO-SURFACE MODEL FOR STEELS WITH YIELD PLATEAU

C.SHEN*, Y.TANAKA**, E.MIZUNO***
and T.USAMI****

The mechanical behavior of the material under cyclic loading is much more compli-
cated than that of monotonic loading. Recently, an attention has been paid to the two-
surface models to predict the behavior of structural steels under cyclic loading. These
models, however, may not give an accurate prediction of the elasto-plastic behavior of
the structural mild steels under cyclic loading. This is because an important feature of
the yield plateau is not treated well. In this paper, a new two-surface model is prop-
osed, by which the cyclic behavior in the yield plateau is accurately predicted. In addi-
tion, a comparison between the experimental data and the prediction by the new model
is shown.

*Keywords* : *plasticity theory, cyclic behavior, stress–strain relationship, two–surface
model, yield plateau*

## 1. INTRODUCTION

Elasto-plastic behavior of structural steel members is a very important factor in design. Generally, under the effect of cyclic loading, the working stress level exceeds the elastic limit and becomes much larger than that specified in the design code. In order to assess the plastic deformation behavior by employing a numerical approach such as finite element method, it is necessary to develop a mechanical model which can represent well a cyclic stress-strain relationship of steel. For example, a local buckling analysis of a thin plate under cyclic loadings requires the development and application of the mechanical model with a better prediction of the plastic behavior.

A good example of mechanical model for steel under cyclic loading is the multi-surface model which was independently developed by Mróz[1],[2] and Iwan[3] in 1967. It includes a finite number of intermediate surfaces with the different plastic hardening moduli and can represent the cyclic characteristics of steel such as the Bauschinger effect. Each intermediate surface moves by the specified hardening rule.

Further, in 1977, Petersson and Popov[4] modified the Mróz multi-surface model by introducing the effective plastic strain and the different hardening rule. This model assumes that the size of each

 * M. Eng., Graduate Student, Dept. of Civil Eng.,
   Nagoya Univ.
   (Chikusaku, Nagoya, Japan)
 ** M. of JSCE, M. Eng., Chubu Electric Power
   Company.
 *** M. of JSCE, Ph. D., Associate Prof., Dept. of Civil
   Eng., Nagoya Univ.
 **** M. of JSCE, D. Sc., D. Eng., Prof., Dept. of Civil
   Eng., Nagoya Univ.

intermediate surface changes by the combination of the weighting function and the initial size of the surface. On the other hand, Minagawa, et al.[5],[6] developed another modified multi-surface model, in which the accumulated effective plastic strain and the effective plastic strain increment were introduced into the Petersson·Popov model as the state varibles to represent the loading history.

On the other hand, a two-surface mode, which consists of only two surfaces such as the yield surface as the inner surface and the bounding surface as the outer surface, is another typical example of cyclic plasticity model. The two-surface model was originally proposed by Dafalias and Popov[7],[8] in 1975 where the plastic modulus in the plastic hardening region is determined by the distance between the current loading point on the yield surface and the conjugate point on the bounding surface. Moreover, in 1983, Tseng and Lee[9] modified the Dafalias·Popov model and demonstrated its efficiency in the one and two dimensional stress state compared with the experimental data.

Many of these multi-surface and two-surface models are aimed at representing stress-strain relations in the hardening region generally and subsequently suitable for prediction of cyclic behavior of the structural steels in a range of relatively large strain. However, when one analyzes the local buckling behavior of SS 400 structural members in a relatively small strain range, it becomes particularly important to check the plastic behavior within the yield plateau under cyclic loading. Therefore it is apparently necessary to develop a suitable mechanical model that can be used to treat the yield plateau. Part of this investigation has already been published in Refs.6)

**Fig.1** Concept of Dafalias・Popov two-surface model



**Fig.2** Test setup

and 10). Specially, various modifications of the original two-surface model, including the treatment of the yield plateau, were proposed in Ref.10) with application to SS 400 steel. In this paper, further modification is presented in order to obtain better prediction for the cyclic behavior of structural steels SS 400, SM 490 and SM 570 in the region of yield plateau as well as of the hardening region. The concept of the virtual bounding line and the movement of the bounding line are introduced in this new model. Further, the model parameters of several structural steels have been determined from the cyclic experimental data and then the experimental results have been compared with the prediction to examine the applicability of the new model.

## 2. REVIEW OF THE DAFALIAS・POPOV TWO-SURFACE MODEL

The Dafalias・Popov two-surface model can be illustrated by using the one-dimensional mechanical behavior of the metal in the plastic hardening region (see **Fig.1**). In this model, the concept of the bounding line (XX′ and YY′ as shown in **Fig.1**) is introduced to describe the plastic behavior of the material under the cyclic loading. It is assumed that the bounding lines have the same slope $E_0^P$ and do not move for any loading path. The distance between these lines is determined by an experiment under monotonic loading. The plastic modulus $E^P$ in the hardening region is assumed to be as follows :

$$E^P = \frac{d\sigma}{d\varepsilon^P} = E_0^P + h\frac{\delta}{\delta_{in} - \delta} \quad \cdots\cdots\cdots\cdots\cdots (1)$$

where $h$ is called the shape parameter, which is a constant during one loading path ; $\delta$ is the distance between the loading point and the bounding line ; $\delta_{in}$ represents the distance between the initial yield point and bounding line during the current loading path.

In addition, there are two more assumptions in

this model : (1) $\delta$ is always not less than zero, further, when $\delta$ becomes zero, it always remains zero throughout the later loading process until unloading starts, and (2) the shape parameter $h$ is a positive number.

Using Eq.(1) and the definition of the bounding line, the relationships between the plastic strain $\varepsilon^P$, the distance $\delta$ and the stress $\sigma$ can be derived as follows : Since the point $(\varepsilon^P, \sigma+\delta)$ always lies on the bounding line, there exists the relationship between the current stress state and the slope of the bounding line :

$$\frac{d(\sigma+\delta)}{d\varepsilon^P} = E_0^P \cdots\cdots\cdots\cdots\cdots\cdots\cdots (2)$$

Substitution of Eq.(1) into Eq.(2) leads to :

$$\frac{d\delta}{d\varepsilon^P} = -h\frac{\delta}{\delta_{in} - \delta} \cdots\cdots\cdots\cdots\cdots\cdots (3)$$

By integrating Eqs.(2) and (3) directly, we get

$$\sigma = \sigma_{in} + E_0^P(\varepsilon^P - \varepsilon_{in}^P) + \delta_{in} - \delta \cdots\cdots\cdots\cdots (4)$$

$$\varepsilon^P - \varepsilon_{in}^P = \frac{\delta_{in}}{h}\left(\frac{\delta}{\delta_{in}} - \ln\frac{\delta}{\delta_{in}} - 1\right) \cdots\cdots\cdots\cdots (5)$$

where $\varepsilon_{in}^P$ and $\sigma_{in}$ are the plastic strain and the stress at the initial yield point during the current loading path (C or F in **Fig.1**). For an arbitrary $\delta$ in nonlinear hardening region, stress and plastic strain can be obtained from Eq.(4) and Eq.(5). It is obvious that the stress calculated by this model never exceeds the bounding line because $\delta$ is always greater than or equal to zero. When the loading point contacts with the bounding line, it will remain on the bounding line until unloading, such as GH shown in **Fig.1**. In this case, the stress is obtained from Eq.(4) for any given plastic strain. On the other hand, the plastic modulus $E^P$ is characterized by the distance $\delta$ and changes from infinity to a constant $E_0^P$ with the decrease in $\delta$. This particular behavior is identical with the

**Table 1** The Contents of the Experiment

| Steel | Specimen | Loading type | Loading history (values of plastic strain(%) at unloading points) |
|---|---|---|---|
| SS400 | SS41-A | ① | monotonic loading in tension up to 4.88% plastic strain |
| | SS41-B | ① | monotonic loading in tension up to 2.48% plastic strain |
| | SS41-C | ② | cyclic loadings in tension up to 2.5% total plastic strain, about 0.05% plastic strain increment allowed for each cycle. |
| | SS41-C | ③ | 0.00,4.04,-0.99,5.02 |
| | SS41-E | ④ | 0.00.39,-0.33,0.39,-0.34,0.39,-0.33,0.39,-0.33,0.39,-0.33,2.01, 1.31,2.01,1.31,2.42 |
| | SS41-F | ④ | 0.00,0.72,-0.68,0.72,-0.68,0.72,-0.70,0.72,-0.68,0.72,-0.69,2.0 |
| | SS41-G | ④ | 0.00,0.55,-0.50,0.55,-0.50,0.54,-0.50,0.54,-0.50,0.56,2.49 |
| | SS41-H | ④ | 0.00,0.48,-0.49,0.48,-0.49,0.48,-0.49,2.48 |
| | SS41-I | ④ | 0.00,0.68,-0.39,0.18,-0.48,0.88,0.73,0.69,0.53,2.48 |
| | SS41-J | ④ | 0.00,0.35,-0.36,0.46,-0.48,0.56,-0.59,0.65,-0.69,2.52 |
| | SS41-K | ④ | 0.00,0.38,-0.88,0.07,-0.36,0.26,-0.89,2.49 |
| | SS41-L | ⑤ | 0.00,0.38,-0.33,2.03,1.32,2.43 |
| | SS41-M | ⑤ | 0.00,0.73,0.68,2.04 |
| | SS41-N | ⑤ | 0.00,0.27,0.02,0.38,0.12,0.53,0.02,0.73,0.12,0.83,0.42,0.9,0.34, 1.04,0.02,2.00 |
| | SS41-O | ⑤ | 0.00,0.55,-0.50,2.53 |
| | SS41-P | ⑤ | 0.00,0.48,-0.49,0.48,-0.49,2.48 |
| | SS41-Q | ⑤ | 0.00,0.58,-0.27,0.69,-0.39,2.48 |
| | SS41-R | ⑤ | 0.00,0.22,-0.23,0.23,-0.22,0.23,-0.22,0.23,-0.23,0.22,-0.22,0.23, -0.22,3.0 |
| | SS41-S | ⑤ | 0.00,0.38,-0.39,0.26,-0.27,0.15,-0.18,0.38,-0.39,2.47 |
| | SS41-T | ⑤ | 0.00,0.88,0.13,0.67,-0.29,2.47 |
| | SS41-U | ⑤ | 0.00,1.22,0.49,1.06,0.70,2.49 |
| | SS41-V | ⑤ | 0.00,0.48,-0.49,2.48 |
| | SS41-W | ⑤ | 0.00,1.22,0.49,2.48 |
| | SS41-X | ⑤ | 0.00,1.08,0.70,2.48 |
| | SS41-Y | ⑤ | 0.00,1.08,0.69,1.09,0.68,1.08,2.48 |
| SM490 | SM50-A | ① | monotonic loading in tension up to 3.69% plastic strain |
| | SM50-B | ② | cyclic loadings in tension up to 2.5% total plastic strain, about 0.05% plastic strain increment allowed for each cycle. |
| | SM50-C | ③ | 0.00,2.96,-1.02 |
| | SM50-D | ④ | 0.00,0.51,-0.84,0.31,-0.51,1.01,0.51,2.49 |
| | SM50-E | ⑤ | 0.00,0.50,0.00,2.47 |
| | SM50-G | ⑤ | 0.00,-0.02,0.50,0.00,0.50,0.00,0.50,0.00,0.50,0.00,2.48 |
| | SM50-F | ⑤ | 0.00,0.40,-0.61,2.00 |
| | SM50-H | ⑤ | 0.00,0.40,-0.39,0.48,-0.50,1.50 |
| | SM50-I | ⑤ | 0.00,0.49,-0.51,0.20,-0.20,0.32,0.00,2.48 |
| | SM50-J | ⑤ | 0.00,0.30,1.69,0.70,1.98,1.49,2.47,1.00,2.95 |
| | SM50-K | ⑤ | 0.00,0.31,0.00,0.60,0.00,0.90,0.00,2.48 |
| | SM50-L | ⑤ | 0.00,-0.60,0.01,-0.61,0.00,-0.60,2.45 |
| SM570 | SM58-A | ① | monotonic loading in tension up to 6.81% plastic strain |
| | SM58-B | ② | cyclic loadings in tension up to 2.5% total plastic strain, about 0.05% plastic strain increment allowed for each cycle. |
| | SM58-C | ③ | 0.00,1.98,-2.68 |
| | SM58-D | ③ | 0.00,-2.04,4.87 |
| | SM58-E | ④ | 0.00,1.98,1.07,2.93,1.48,2.93,1.98,2.75,0.74,3.87,3.01,3.83,3.27, 4.41,2.57,4.77 |
| | SM58-F | ④ | 0.00,0.29,0.38,1.00,-0.50,1.91,1.12,2.87,-1.03,-0.51,-0.32,3.88 |
| | SM58-G | ④ | 0.00,-0.02,0.50,0.00,0.58,-0.01,0.59,0.00,1.82,1.25,2.48,1.42,2.99, 2.04,2.98,2.04,3.45 |
| | SM58-H | ④ | 0.00,4.07,1.01,4.06 |
| | SM58-I | ④ | 0.00,0.58,-0.63,0.78,-0.83,1.17,-1.23,1.93,0.99,2.90,1.13,3.87 |
| | SM58-J | ④ | 0.00,0.49,-1.54,-1.39,-1.31,-0.96,-1.85,1.58,0.66,2.50,1.1,2.22, 1.35,2.99,2.33,3.87 |

observation in experiments.

# 3. EXPERIMENTS OF STRUCTURAL STEELS SS 400, SM 490 AND SM 570

The Dafalias · Popov two-surface model is easy to use in uniaxial cyclic loading problems. But in many cases, it can not given a good prediction of the cyclic behavior of steel with yield plateau that is an important feature of the structural steels. In order to develop a new two-surface model, which can give an accurate prediction in most cases, a series of experiments of structural steels SS 400, SM 490 and SM 570 were carried out under cyclic loadings. The test machine used is the MTS 810 (Material Test System) with 25 tonf loading capacity (see **Fig.2**).

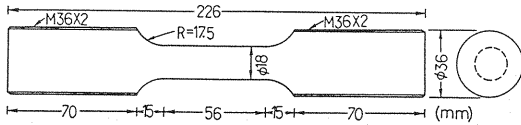The contents of the experiment are shown in **Table 1**. Only one type of the test specimen shown
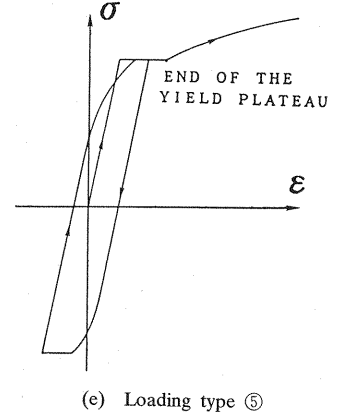
Fig.3 Dimension of test specimen



(a) Loading type ①



(b) Loading type ②



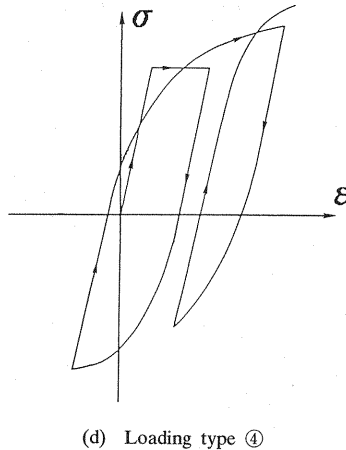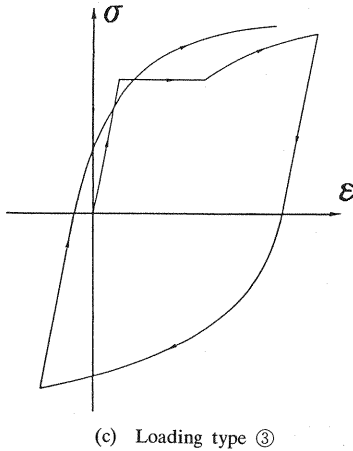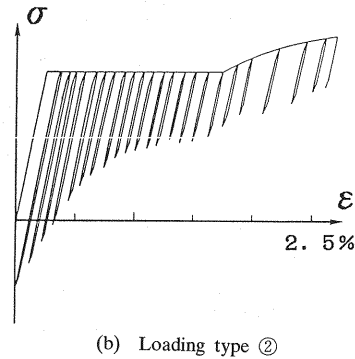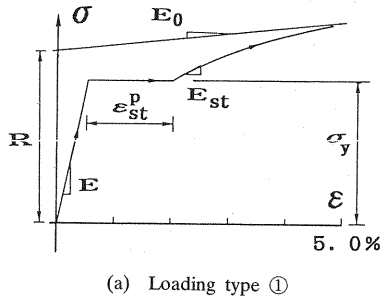(c) Loading type ③



(d) Loading type ④



(e) Loading type ⑤

Fig.4 Loading type of the experiment

in **Fig.3** is used throughout the whole experiments. To prevent the effects of the load eccentricity and imperfection, the specimens are made into a solid circular section and the length of uniform section is 56 mm. Testing is conducted at a very lower controlled strain rate of about $10^{-4}$ (mm/mm)/sec. The strain is measured with a contact displacement gauge of length 50 mm attached on the specimen. Moreover, the experimental data are recorded by a computer and the stress-strain curve is drawn on the screen simultaneously. In order to get sufficient experimental data for establishing a new model, the following five loading types are adopted in the test and schematically shown in **Fig.4**.

Type ① : Monotonic loading experiment in tension is conducted approximately up to 5% strain (as shown in **Fig.4** (a)). These experimental data

are used to determine Young's modulus $E$, Poisson's ratio $\nu$, yield stress $\sigma_y$, length of yield plateau $\varepsilon_{st}^P$, slope of bounding line $E_0^P$, initial height of the bounding lines $R$ and the plastic modulus $E_{st}^P$ at the initial linear hardening.

Type ② : A cyclic loading experiment is carried out to measure the change in the elastic range between each successive loading cycles. **Fig.4** (b) shows a typical stress-strain relationship in the experiment. About 0.05% plastic strain is allowed for each loading cycle and the cycles are repeated until about 2.5% total plastic strain is achieved. For each loading cycle in **Fig.4** (b), the initial yield point is assumed to be the point at which the slope of the stress-strain curve deviates by 1% from the initial slope at unloading stage. The elastic range of each cycle is measured as a distance from the

**Fig.5** Concept of the accumulated effective plastic strain



(a) The reduction in elastic range of steel SS 400



(b) The reduction in elastic range of steel SM 490



(c) The reduction in elastic range of steel SM 570

**Fig.6** The reduction in elastic range
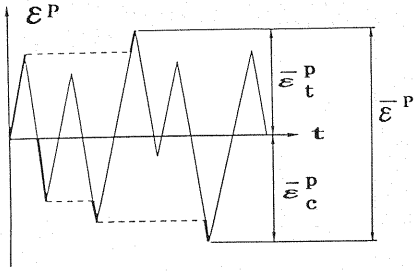
unloading point to the initial yield point.

Type ③ : One cycle loading experiment including tension and compression is conducted in which about 5% plastic strain range is allowed. The shape parameter $h$ is determined using the method described in Ref.10) with these experimental results (shown in **Fig.4** (c)).

Type ④ : Random cyclic loading experiments are implemented for comparison between the experimental and simulated results (see **Fig.4** (d)).

Type ⑤ : Cyclic loadings are conducted to observe the reduction in the yield plateau. Several loading cycles are carried out before the yield plateau disappears (see **Fig.4** (e)).

## 4. EXPERIMENTAL OBSERVATIONS AND PROPOSAL OF A NEW TWO-SURFACE MODEL

In this section, based on the experimental observations of SS 400, SM 490 and SM 570 steel specimens, a new modified two-surface model is proposed. At the same time, a comparison between the prediction by the proposed model and the experimental results is also presented.

**( 1 ) Reduction in the Elastic Range**

It was found that the elastic range $\kappa$ is not constant under cyclic loading (Ref.10). For steels SS 400, SM 490 and SM 570, the elastic range becomes smaller as the plastic deformation increases. For example, the rapid reduction in the elastic range occurs only within 0.3% plastic strain. Beyond an approximately 1% plastic deformation, the elastic range no longer changes so significantly, which is known as the steady state.

To represent the reduction of the elastic range, a concept of the accumulated effective plastic strain[6] $\bar{\varepsilon}^P$ is introduced. It is schematically illustrated in **Fig.5**, where only the bold parts are added to $\bar{\varepsilon}^P$. The accumulated effective plastic strain represents the maximum range of the plastic strain that the material has ever experienced in both compression and tension. According to the results of experiment type ② (see **Fig.4** (b)), the reduction of the elastic
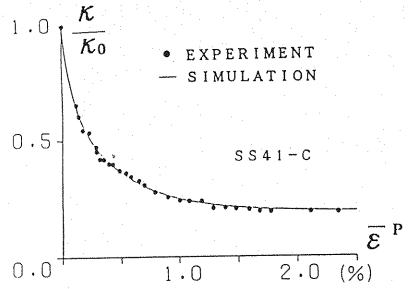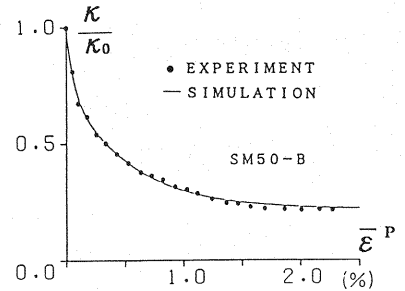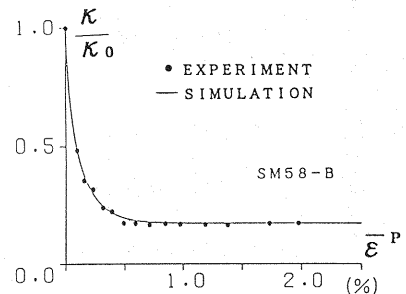
range $\kappa$ can be expressed as follows :

$$\kappa/\kappa_0 = \alpha - a \cdot \exp(-b\bar{\varepsilon}^P \times 100)$$
$$- (\alpha - a - 1)\exp(-c\bar{\varepsilon}^P \times 100) \cdots\cdots(6)$$

where $a$, $b$ and $c$ are the constants and determined in terms of the experimental results of type ② using the least square method. From Eq.(6), it can be seen that when $\bar{\varepsilon}^P = 0$, $\kappa = \kappa_0$ (the initial size of the elastic range, i.e., $\kappa_0 = 2\sigma_y$) ; when $\bar{\varepsilon}^P = \infty$, $\kappa = \alpha \cdot \kappa_0$ (the elastic range of the steady state). Since the accumulated effective plastic strain depends on the loading history, it is suitable to describe the plastic behavior of material.

The relationships between reduction of the elastic range $\kappa/\kappa_0$ and accumulated effective plastic strain $\bar{\varepsilon}^P$ for each steel type SS 400, SM 490 and SM 570 are obtained from the results of experiment type ② and are shown in **Fig.6**. The values of $a$, $b$,
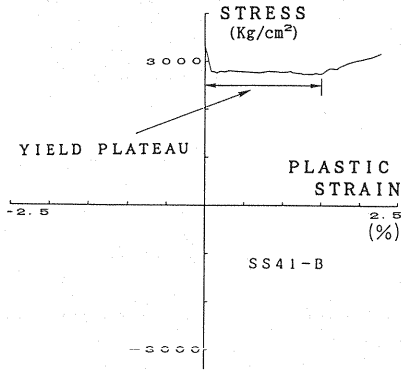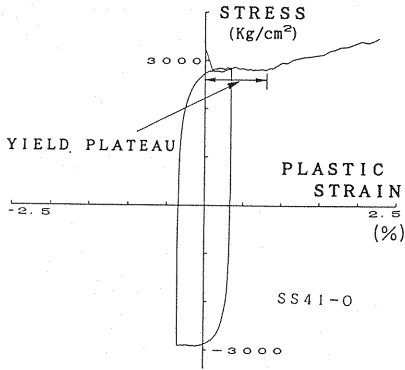
Fig.7 The yield plateau in monotonic loading
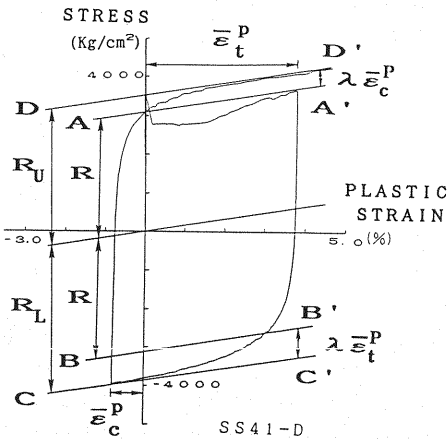


Fig.8 The yield plateau in cyclic loading



Fig.9 Movement of the bounding line

$c$, and $\alpha$ calibrated are listed in **Table 2** (in section 6).

### ( 2 ) Modification of Shape Parameter $h$

The shape parameter $h$ in Eq.(1) affects the curvature of stress-strain curve in the non-linear hardening region CD or FG in **Fig.1**. It was assumed to be a constant during one loading path in the Dafalias・Popov two-surface model. But the experimental results in Ref.10) indicate that $h$ changes with $\delta$ and stress-strain curve is sensitive to this parameter. As a result, a linear relationship between $h$ and $\delta$ has been adopted in Ref.10).

$$h = d\delta + e \quad \cdots\cdots\cdots\cdots\cdots\cdots\cdots\cdots\cdots\cdots\cdots\cdots\cdots(7)$$

where $d$ and $e$ are the constants. They are determined with the experimental results obtained from the experiment of type ③ as mentioned in Ref.10). Substituting Eq.(7) for $h$ in Eq.(3) and integrating Eq.(3), one obtains the following relationship between plastic strain and $\delta$.

$$\varepsilon^P - \varepsilon_{in}^P = \frac{\delta}{\delta_{in}} \ln\left(\frac{d\delta + e}{d\delta_{in} + e} \cdot \frac{\delta_{in}}{\delta}\right) + \frac{1}{d}\ln\left(\frac{d\delta + e}{d\delta_{in} + e}\right)$$
$$\cdots\cdots\cdots\cdots\cdots\cdots\cdots\cdots\cdots\cdots\cdots(8)$$

The values of $d$ and $e$ calibrated with the results of experiment type ③ are listed later in **Table 2**.

### ( 3 ) Treatment of the Yield Plateau

Many structural steels are featured by the yield plateau. However, it has not been treated well in many cases especially under cyclic loading condition. In the monotonic loading experiment of SS 400 steel (see **Fig.7**), the yield plateau occurs when the stress reaches the yield point and the length of the yield plateau is a constant for each material. However, in the cyclic loading experiment, the length of the yield plateau decreases if cyclic loadings are carried out within the yield plateau (see **Fig.8**). According to the experimental fact reported in Ref.10), it has been found that the disappearance of the yield plateau depends on the plastic work and the accumulated effective plastic strain. Considering the monotonic loading case, the relationship between the plastic work and the accumulated effective plastic strain at the terminal point of the yield plateau is assumed as follows :

$$\frac{\bar{\varepsilon}^P}{\varepsilon_{st}^P} - 1 = M \cdot \left(\frac{W^P}{W_{st}^P} - 1\right) \cdots\cdots\cdots\cdots\cdots\cdots(9)$$

where $\varepsilon_{st}^P$ and $W_{st}^P$ represent the plastic strain and plastic work at the end of the yield plateau under monotonic loading respectively ; $W^P$ is the plastic work given by $\int \sigma d\varepsilon^P$ ; $M$ is a material parameter determined by the least square method according to the results of the experiment type ⑤. For steels SS 400 and SM 490, the values of $M$ are found to be $-0.370$ and $-0.0522$ respectively. The yield plateau in steel SM 570 is too short to be measured so that it is negligible in prediction. It is noted that once Eq.(9) is satisfied by the accumulated effective plastic strain $\bar{\varepsilon}^P$ and the plastic work $W^P$, the yield plateau disappears forever. On the other hand, when the stress is on the yield plateau, the equations (4) and (8) can not be used in the stress and plastic strain relation. Moreover, the constant
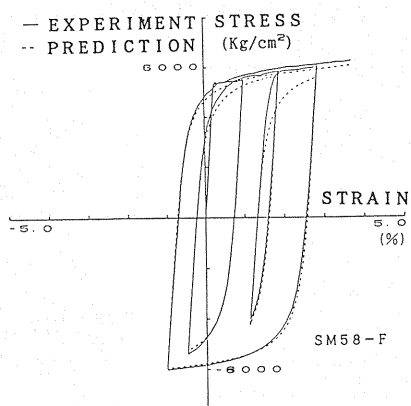
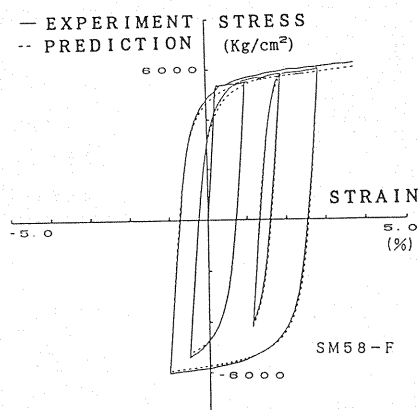Fig.10 Prediction without virtual bounding line

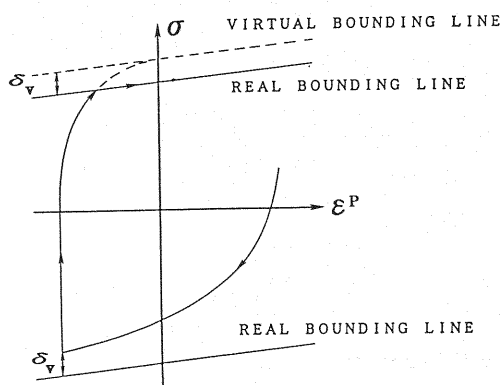Fig.12 Improved prediction with virtual bounding line

Fig.11 Concept of the virtual bounding line

**Table 2** Material Parameters of Steels SS 400, SM 490 and SM 570

| Material | S S 4 0 0 | S M 4 9 0 | S M 5 7 0 |
|---|---|---|---|
| $E$ | $2.11 \times 10^6$ | $2.10 \times 10^6$ | $2.20 \times 10^6$ |
| $\sigma_y$ | $2.80 \times 10^3$ | $3.64 \times 10^3$ | $5.35 \times 10^3$ |
| $\varepsilon_{st}^P$ | $1.53 \times 10^{-2}$ | $1.24 \times 10^{-2}$ | $0.00$ |
| $\nu$ | $0.290$ | $0.247$ | $0.252$ |
| $E_{st}^P /E$ | $2.49 \times 10^{-2}$ | $3.4 \times 10^{-2}$ | $1.02 \times 10^{-2}$ |
| $E_0^P /E_{st}^P$ | $0.361$ | $0.411$ | $0.490$ |
| $R / \sigma_y$ | $1.15$ | $1.06$ | $1.05$ |
| $\lambda /E_0^P$ | $0.802$ | $0.538$ | $1.003$ |
| a | $-0.505$ | $-0.528$ | $-0.553$ |
| b | $2.17$ | $1.88$ | $6.47$ |
| c | $14.4$ | $18.7$ | $34.8$ |
| $\alpha$ | $0.191$ | $0.217$ | $0.175$ |
| d | $5.00 \times 10^2$ | $3.16 \times 10^2$ | $1.04 \times 10^3$ |
| e /E | $0.30$ | $0.484$ | $0.361$ |
| M | $-0.37$ | $-0.0522$ | |

plastic modulus $E_{st}^P$ will be used from the end of the yield plateau to the unloading point.

**( 4 ) Movement of the Bounding Line**

The bounding lines used in the Dafalias · Popov two-surface model are assumed to be a pair of fixed parallel lines. However, from the experimental result of Specimen SS 41-D (shown in **Fig.9**), the initial bounding line of the first tension loading may be defined to be the line AA′ and then the bounding line in the compression side is supposed to be the line BB′ if the unchangeable bounding lines are used. However, test curve from tension to compression in **Fig.9** exceeds BB′ and approaches the line CC′. Moreover, in the next loading from compression to tension, the stress-strain curve approaches the line DD′ instead of AA′. In the present model, the accumulated effective plastic strain $\bar{\varepsilon}_t^p$ in tension side and $\bar{\varepsilon}_c^p$ in compression side (as shown in **Fig.5**) are used to describe the movements of the lower and upper bounding lines respectively. The new positions of the two bounding lines are thus expressed as follows.

$$R_U = R + \lambda \bar{\varepsilon}_c^p \qquad R_L = R + \lambda \bar{\varepsilon}_t^p \cdots\cdots\cdots (10)$$

where $R_U$ and $R_L$ represent the heights of the upper and lower bounding lines from the origin respectively ; $R$ is the initial height of the bounding lines and $\lambda$ is a material parameter determined by the experiment type ③. The value of $R$ and $\lambda$ for steels SS 400, SS 490 and SM 570 are shown in **Table 2** later. From Eq.(10), it may be seen that the expansion of the bounding lines is not isotropic when $\bar{\varepsilon}_c^p$ and $\bar{\varepsilon}_t^p$ are not the same.

**( 5 ) Proposal of the Virtual Bounding Line Concept**

It is seen in **Fig.10** that when the unloading point does not match the bounding line, the predicted curve of the next loading path given by Eq.(8) and Eq.(4) bends relatively earlier than the experimental curve near the bounding line. In order to avoid such earlier bending of the stress-strain curve, a new concept of the virtual bounding line is proposed (see **Fig.11**). It is assumed that the virtual bounding line is parallel to the real bounding line and shifted by a distance $\delta_V$ up or down with respects to tension and compression
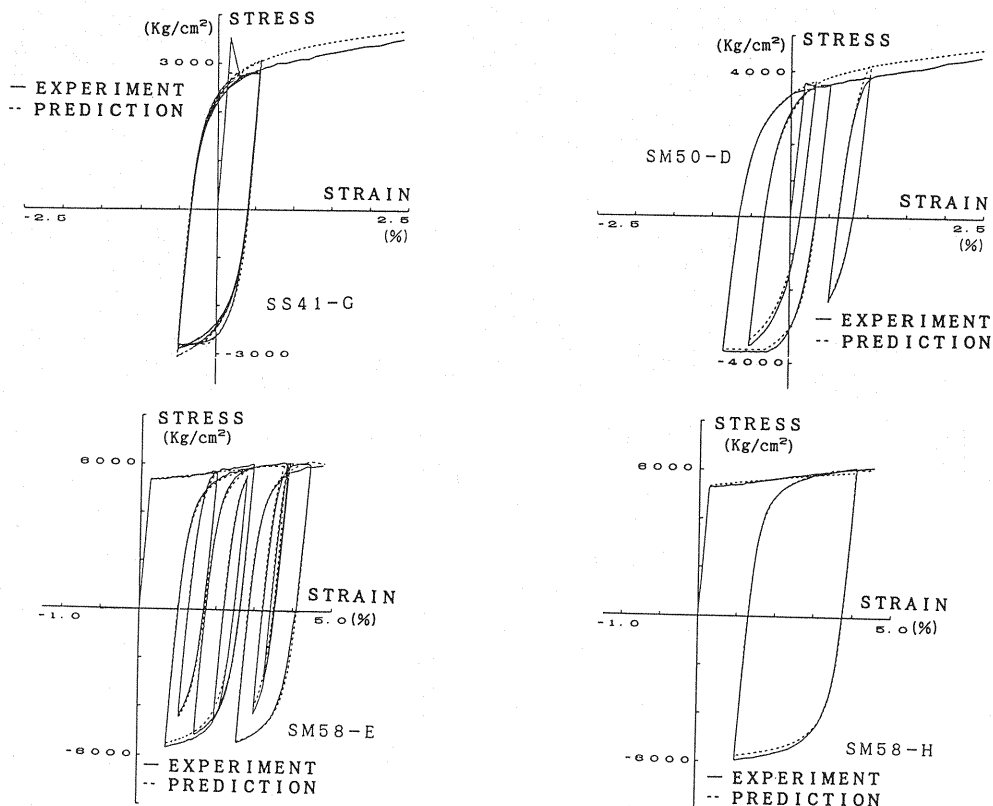
**Fig.13**  Comparison between the experimental and the numerical results

parts, where $\delta_v$ is the $\delta$ of the latest unloading point during last loading cycle. In such a case, the distance $\delta$ used in Eq.(8) is measured from the virtual bounding line. It should be noted that the virtual bounding line is used only after the yield plateau disappears and only for those loading points inside the two real bounding lines. If the loading point reaches the real bounding line, $\delta$ is assumed to be zero until unloading. In the first loading path, the virtual bounding line is defined to coincide with the real bounding line. With the introduction of the virtual bounding lines, improved prediction is obtained as shown in **Fig.12**.

**( 6 )  Examples**

Some examples of the comparsion between test and prediction for three kinds of steels are shown in **Fig.13**. The applicability and accuracy of the proposed model may be demonstrated by these examples. The material parameters used in the model are shown in **Table 2**.

## 5.  The Proposed Model Versus Other Two-surface Models

Several two-surface models have been proposed by other researchers. A comparison between the Dafalias・Popov model[7),8)], the Tseng・Lee mod-

el[9)], the Cofie・Krawinkler model[11)] and the proposed model is given in **Table 3**.

It is noted that the two-surface model previously proposed by the authors[10)] is different from the present model in that the movement of the bounding lines is newly introduced.

## 6.  CONCLUSIONS

The proposed model in this paper may be used to predict the elasto-plastic behavior of structural steels under the cyclic loadings both with and without yield plateau. Only a few experiments are required to determine the model parameters (see **Table 2**). Through the experimental study and the numerical simulation of uniaxial behavior of the structural steels, the following conclusions are drawn :

(1)  The elastic stress range decreases as the accumulated effective plastic strain increases. But, beyond about 1% plastic strain, the elastic range remains constant.

(2)  The length of the yield plateau is not the constant under cyclic loading. It decreases with the increase in plastic work.

(3)  The prediction using the shifted bounding lines is better than that using fixed lines. The

**Table 3** Comparison between the Two-surface Models

| Model | Dafalias · Popov Refs. 7,8) | Tseng · Lee Ref. 9) | Cofie · Krawinkle Ref. 11) | Proposed |
|---|---|---|---|---|
| Size in elastic range | constant | $\kappa / \kappa_{\square} = \alpha +$ $(1- \alpha)EXP(-W^P/4)$ $W^P$: plastic work | constant | changes with the accumulated effective plastic strain |
| Hardening rule of yield surface | kinematic hardening | combined hardening | kinematic hardening | combined hardening |
| Bounding surface (line) | constant in size and moves with $d \varepsilon^P$ | isotropically expands with $\lvert \sigma \rvert_{max}$ | constant in size and moves with mean stress $\sigma_m$, etc. | changes in size, moves with $d \varepsilon^P$ |
| Shape parameter | changes with $\delta_{in}$ | constant | changes with $\delta_{in}$ | changes with $\delta$ linearlly |
| Advantage | simple and only a few parameters required | has been extended to the multi-axial case. | accurate for mild steel under cyclic loading in strain hardening | applicable to treat yield plateau under cyclic loading, only a few experiments are required to determine parameters |
| Limitation | · only suitable for prediction with moderately large plastic strain · unapplicable for predicting cyclic behavior in yield plateau | · not clear in determination of h · unapplicable for predicting cyclic behavior in yield plateau | · too many parameters and experiments required · unapplicable for predicting cyclic behavior in yield plateau | · not yet extended to multi-dimensional case |

movemetn of the bounding line may be defined as the function of the accumulated effective plastic strains in tension and compression side.

(4) The introduction of the virtual bounding line can overcome the earlier bending of the predicted curves when the unloading point does not match the bounding line.

In summary, the comparison between the experimental and analytical results shows that the proposed model may be accurate in predicting the elasto-plastic behavior of steel under cyclic loading.

## REFERENCES

1) Mróz, Z. : On the description of anisotropic work hardening, J. Mech. Phys. Solids, Vol.15, pp.163~175, 1967.

2) Mróz, Z. : An attempt to describe the behavior of metal under cyclic loading using a more general work hardening model, Acta Mechanica, Vol.7, pp.199~212, 1969.

3) Iwan, W.D. : On a class of model for the yielding behavior of continuous and composite system, Trans. ASME, J. Appl. Mech., pp.612~617, Sept. 1967.

4) Petersson, H. and Popov, E.P. : Constitutive relation for generalized loadings, Proc. of ASCE, Vol.104, No. EM4, pp.611~627, 1977.

5) Minagawa, M., Nishiwaki, T. and Masuda, N. : Modelling cyclic plasticity of structural steels, Structural Eng. / Earthquake Eng., Vol.4, No.2, pp.361s~370s, Oct. 1987.

6) Minagawa, M., Nishiwaki, T. and Masuda, N. : Prediction of uni-axial cyclic plasticity behaviors of structural steel in plastic flow region, Journal of Structural Engineering, Vol.35A, pp.53~65, 1989. (in Japanese).

7) Dafalias, Y.F. and Popov, E.P. : A model of nonlinear hardening materials for complex loading, Acta, Mech., Vol.21, pp.173~192, 1975.

8) Dafalias, Y.F. and Popov, E.P. : Plastic internal variables

formalism of cyclic plasticity, Trans. ASME, J. Appl. Mech., pp.645~651, Dec., 1975.

9) Tseng, N.T. and Lee, G.C. : Simple plasticity model of two-surface type, Journal of Engineering Mechanics, Proc. ASCE, Vol.109, No.3, pp.795~810, June 1983.

10) Tanaka, Y., Mizuno, E., Shen, C. and Usami, T. : Development of a cyclic two-surface model with yield plateau, Journal of Structural Engineering, Vol.37A, pp.1 ~14, March, 1991. (in Japanese).

11) Cofie, N.G. and Krawinkler, H. : Uniaxial cyclic stress-strain behavior of structural steel, Journal of Engineering Mechanics, Proc. ASCE, Vol.111, No.9, pp.1105~1120, Sept. 1985.

12) Sugiura, K. : Low-cyclic fatigue of structural steel, p.191, A dissertation submitted to the faculty of the graduate school of the State University of New York at Buffalo in partial fulfilment of the requirement of the degree of Doctor of Philosophy, Sept. 1988.